Supplementary Materials

Simulating solid-electrolyte-interphase formation spanning 10^8 time scales with atomically informed phase-field model

Kena Zhang[1,+], Yanzhou Ji[1,+,§], Qisheng Wu[2], Seyed Amin Nabavizadeh[1], Yue Qi[2,*] and Long-Qing Chen[1,*]

[1]*Department of Materials Science and Engineering, The Pennsylvania State University, University Park, PA 16802, USA*

[2]*School of Engineering, Brown University, Providence, RI 02912, USA*

Table S1 Standard reduction potentials, Gibbs free energy releases, and activation energies for the 10 (electro)chemical reactions from atomistic simulations. All parameters are calculated by DFT.

Index	Reaction	ψ_m^0 (V, w.r.t. SHE)	ΔG_m^0 (eV)	ΔG_m^* (eV)
0	$Li^+ + e^- = Li$	-3.04		--
1	$EC + e^- = o\text{-}EC^-$	-2.18		0.03
2	$o\text{-}EC^- + Li^+ = Li^+/o\text{-}EC^-$	N/A	-1.30	0
3	$EC + Li^+ = Li^+/c\text{-}EC$	N/A	-0.38	0
4	$Li^+/c\text{-}EC + e^- = Li^+/o\text{-}EC^-$	-1.26		0.05
5	$o\text{-}EC^- + e^- = CO_3^{2-} + C_2H_4$	-1.26		0.92
6	$CO_3^{2-} + 2Li^+ = Li_2CO_3$	N/A	-4.43	0
7	$CO_3^{2-} + Li^+ = Li^+/CO_3^{2-}$	N/A	-2.34	0
8	$Li^+/CO_3^{2-} + Li^+ = Li_2CO_3$	N/A	-2.09	0
9	$Li^+/o\text{-}EC^- + e^- = Li^+/CO_3^{2-} + C_2H_4$	-0.21		0.72
10	$Li^+/o\text{-}EC^- = \frac{1}{2}Li_2BDC$	N/A	-1.69	0.15[1]
11	$Li^+/o\text{-}EC^- + Li^+ = 2Li^+/o\text{-}EC^-$	N/A	0.67	0
12	$\frac{1}{2}Li_2BDC + e^- + Li^+ = Li_2CO_3 + C_2H_4$	-0.21	-0.4	0.17

Table S2 Standard reduction potentials, Gibbs free energy releases, and activation energies for R1 to R3 from atomistic simulations. All parameters are calculated by DFT.

Index	Reaction	ψ^0 (V, w.r.t. SHE)	ΔG^0 (eV)	ΔG^* (eV)	k_m (1/s)
R0	$\mathrm{Li^+ + e^- = Li}$	-3.04			0.18[2]
R1	$\mathrm{Li^+ + e^- + EC = \frac{1}{2}Li_2BDC}$	-2.18	-2.99	0.15	1.90×10^{10}
R2	$\mathrm{\frac{1}{2}Li_2BDC + Li^+ + e^- = Li_2CO_3 + C_2H_4}$	-0.21	-0.4	0.17	8.76×10^{9}
R3	$\mathrm{2Li^+ + 2e^- + EC = Li_2CO_3 + C_2H_4}$	0.65	-3.39	0.72	5.14

Table S3 Parameters used in phase-field simulations

Parameters	Symbol	Value [Unit]	Source
Gradient energy coefficient	κ_E, κ_M, κ_{S1}, κ_{S2}	7.5×10^{-10} [J/m]	Calculated
Barrier heights of the double well	w_E, w_M, w_{S1}, w_{S2}	4×10^{9} [J/m^3]	Calculated
	γ_{jl}	4×10^{9} [J/m^3]	Calculated
Bulk concentration of Li$^+$	c_0	1 M	
Site density of electrode	$c_{Li^0}^{M}$	81.8 M	
Li site density of Li_2CO_3	$c_{Li^+}^{S1}$	57 M	
Li site density of Li_2BDC	$c_{Li^+}^{S2}$	13.5M	
EC-related group side density of electrode	c_{EC}^{M}	0 M	
EC-related group side density of Li_2CO_3	c_{EC}^{S1}	57 M	
EC-related group side density of Li_2BDC	c_{EC}^{S2}	13.5 M	
Li$^+$ diffusion coefficient in electrolyte	$D_{Li^+}^{E}$	3.5×10^{-10} [m^2/s]	MD
Li$^+$ diffusion coefficient in electrode	$D_{Li^+}^{M}$	0	
Li$^+$ diffusion coefficient in Li_2CO_3	$D_{Li^+}^{S1}$	1.1×10^{-11} [m^2/s]	[3]
Li$^+$ diffusion coefficient in Li_2BDC	$D_{Li^+}^{S2}$	1.0×10^{-10} [m^2/s]	Estimated
EC diffusion coefficient in electrolyte	D_{EC}^{E}	6.8×10^{-10} [m^2/s]	MD
EC diffusion coefficient in electrode	D_{EC}^{M}	0	
EC diffusion coefficient in Li_2CO_3	D_{EC}^{S1}	0	
EC diffusion coefficient in Li_2BDC	D_{EC}^{S2}	1×10^{-10} [m^2/s]	Estimated
Electron tunneling barrier in Li_2CO_3	$\Delta E_{Li_2CO_3}$	1.78 [eV]	[4]
Electron tunneling barrier in Li_2BDC	ΔE_{Li_2BDC}	0.24 [eV]	Estimated
Interfacial energies	ε	0.5 [J/m^2]	[5]
Interface thickness	L	1 [nm]	

Note: The Gradient energy coefficient is calculated by $\frac{3}{2}\varepsilon L$, and the barrier heights of the double well are calculated by $\frac{8\varepsilon}{L}$. γ_{jl} are assumed to be the same as the barrier heights of the double well

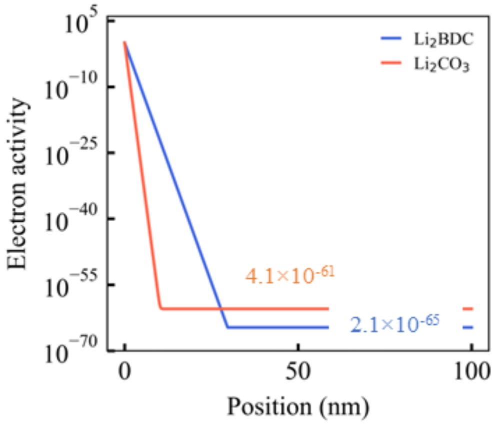

Fig. S1 Spatial distribution of electron concentration due to electron tunneling. Based on equation 1 and equation 2, the equilibrium activity of electrons for R1 and R3 are 2.1×10^{-65} and 4.1×10^{-61}, respectively.

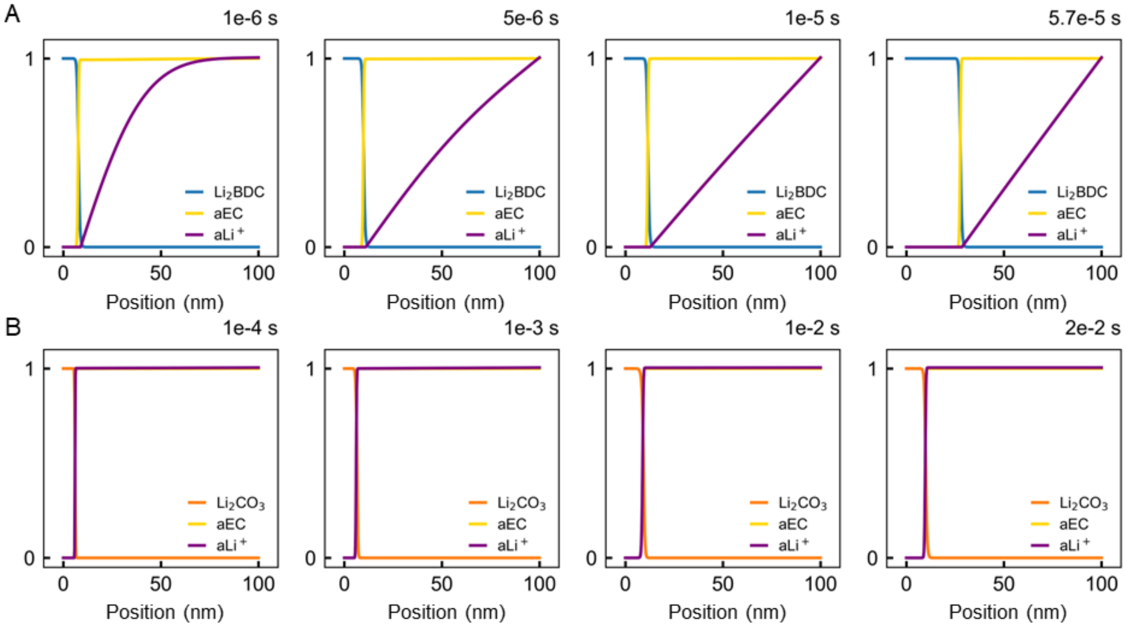

Fig. S2 Temporal evolution of the order parameters and the distribution of species Li^+ and EC at 4 selected time points for (A) organic Li_2BDC via R1 and (B) inorganic Li_2CO_3 via R3. The position (0 ~ 100 nm) signifies the distance from the Li anode surface to the electrolyte region. There is no gradient in activity of EC during both organic and inorganic SEI growth, indicating that EC molecules could be reduced in site without requiring additional EC compensated from the electrolyte. In contrast, during organic SEI growth, a gradient of aLi^+ within the electrolyte is evident. This indicates that the formation of organic SEI necessitates the diffusion of species Li^+ from the bulk electrolyte to the reaction interface. The simulation corresponds to case (4) in the section of 'Effect of Li^+ and EC molecules on SEI formation rates' in the main text. *Evolving both Li^+ and EC* ($a_{Li^+} \neq 1$ and $a_{EC} \neq 1$ calculated by equation 9) indicates that both Li^+ and EC are consumed according to their stoichiometric ratio during SEI growth, and their concentration distributions over time are determined by the diffusion equation.

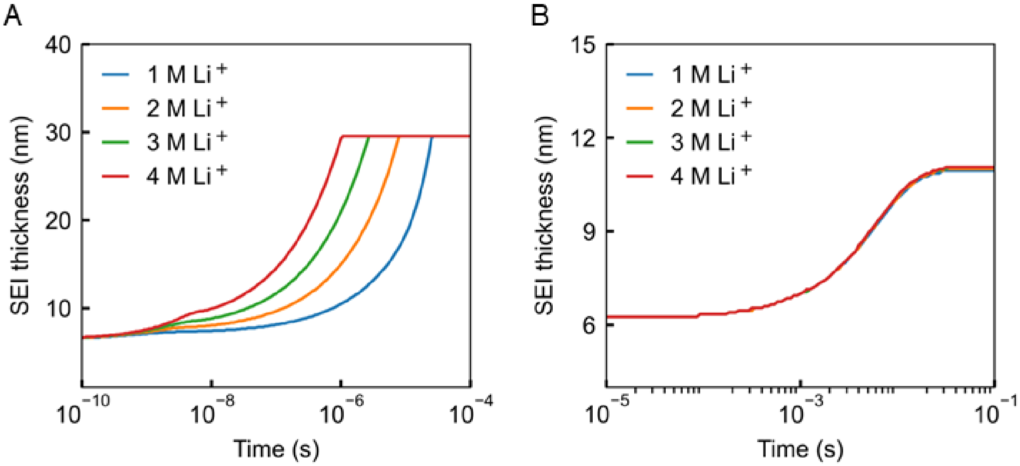

Fig. S3 Thickness evolution of dense (A) Li_2BDC via R1 and (B) Li_2CO_3 via R3 under different Li^+ concentrations.

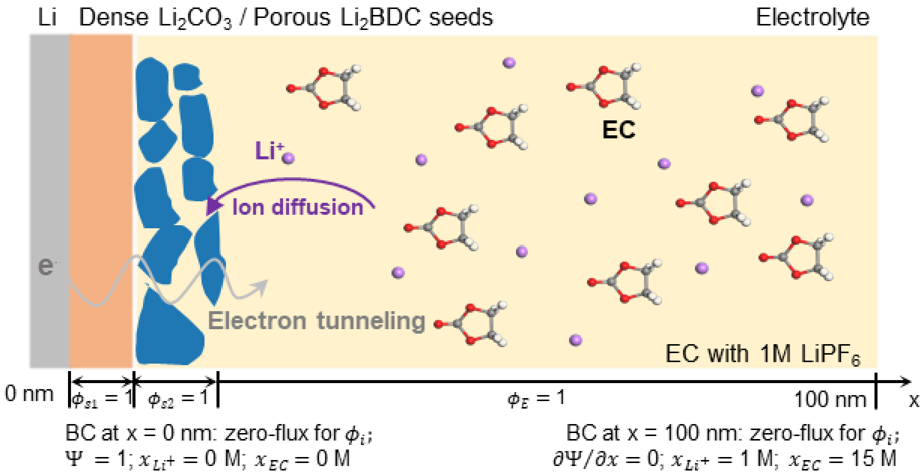

Fig. S4 1D phase field simulation system with a two-layer initial SEI seeds and boundary conditions. There is a two-layer structured SEI nucleus within the simulation system, comprising a 0.5 nm of dense Li_2CO_3 layer adjacent to the Li metal and 6 nm thick of Li_2BDC at the outer layer with a porosity of 50%.

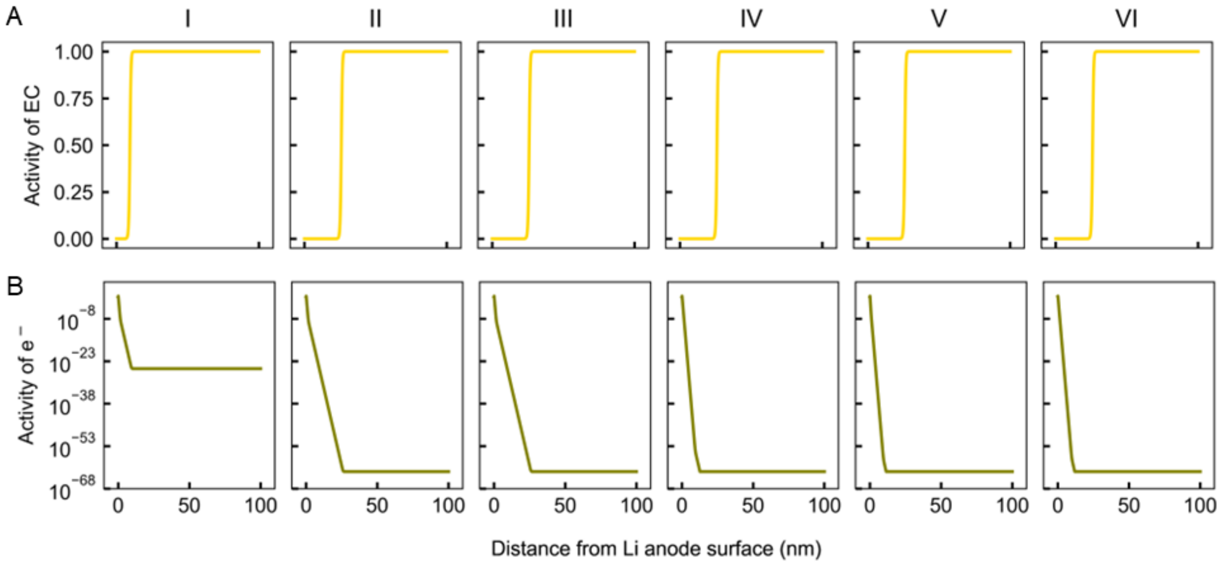

Fig. S5 Temporal evolution of the activity of EC and electrons at 6 selected time points at Fig. 4a.

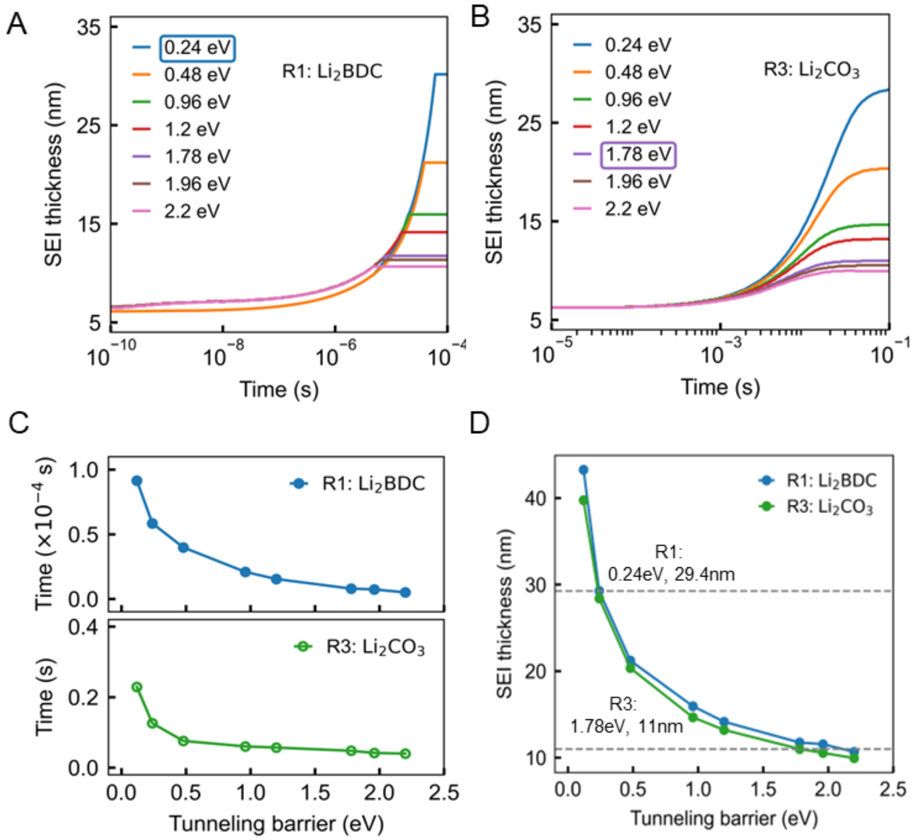

Fig. S6 Effect of electron-tunneling barrier ΔE on SEI growth. Thickness evolution of (A) dense organic Li_2BDC via R1 and (B) dense inorganic Li_2CO_3 via R3. (C) The time required to reach the tunneling-limited thickness as a function of ΔE. (D) Comparison of the final thickness of Li_2BDC and Li_2CO_3. The tunneling barriers are set as 0.24 eV (estimated) for Li_2BDC and 1.78 eV (DFT) for Li_2CO_3, and a series of parameterized values are explored around these baselines to evaluate the impact of ΔE on SEI growth dynamics.

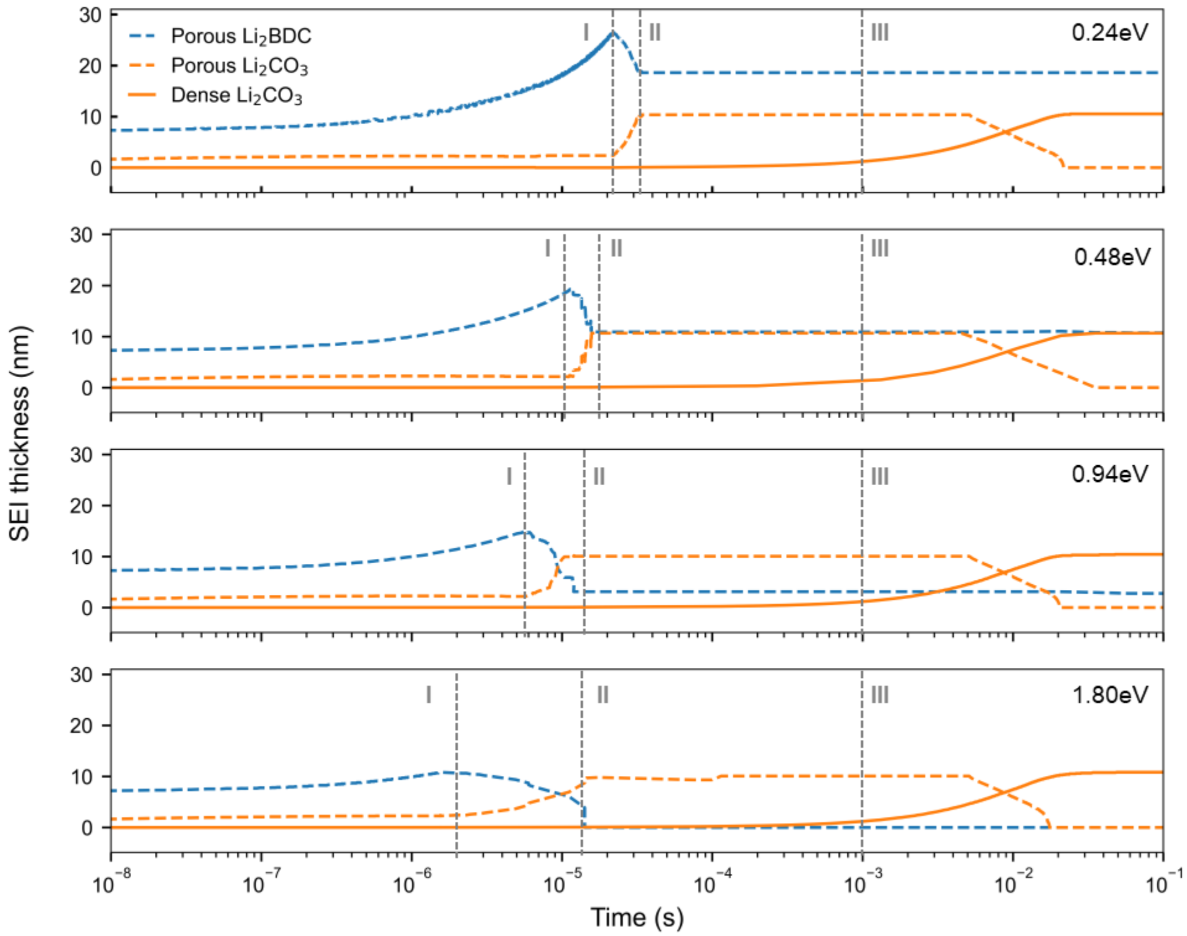

Fig. S7 Time-resolved SEI growth via R1 to R3 in the Li/(EC + 1 M $LiPF_6$) system with varying electron tunneling barriers for Li_2BDC. The electron-tunneling barrier for crystalline Li_2CO_3 is fixed at 1.78 eV, while that for Li_2BDC varies from 0.24, 0.48, 0.94 to1.80 eV. The dashed and solid lines represent the porous and dense products, respectively. Stage I: Porous organic Li_2BDC forms via R1; State II: A portion of this Li_2BDC is converted to porous inorganic Li_2CO_3 through the R2 pathway. Stage III: The remaining pores are filled as additional Li_2CO_3 is produced by the direct two-electron reduction of EC via R3.

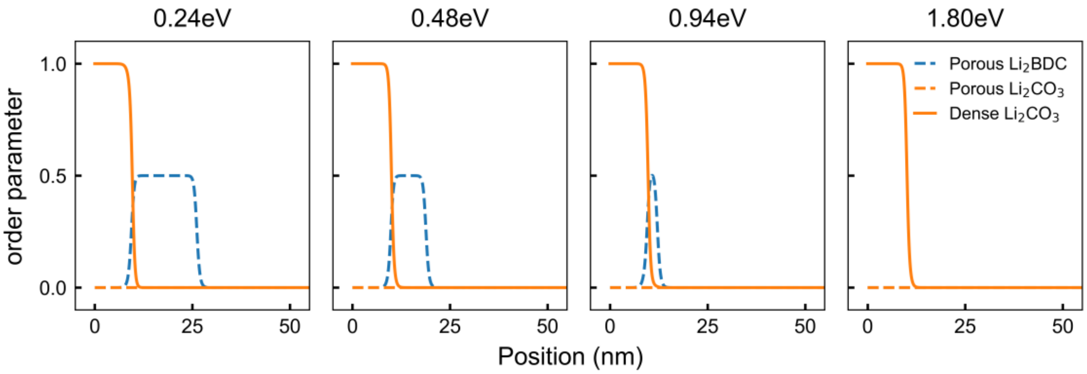

Fig. S8 Spatial distribution of phase-field order parameters at *t* = 0.1 s for varying electron tunneling barriers of Li_2BDC. The position (0 ~ 50 nm) signifies the distance from the Li anode surface to the electrolyte region. The order parameters distinguish the organic Li_2BDC and inorganic Li_2CO_3 phases.

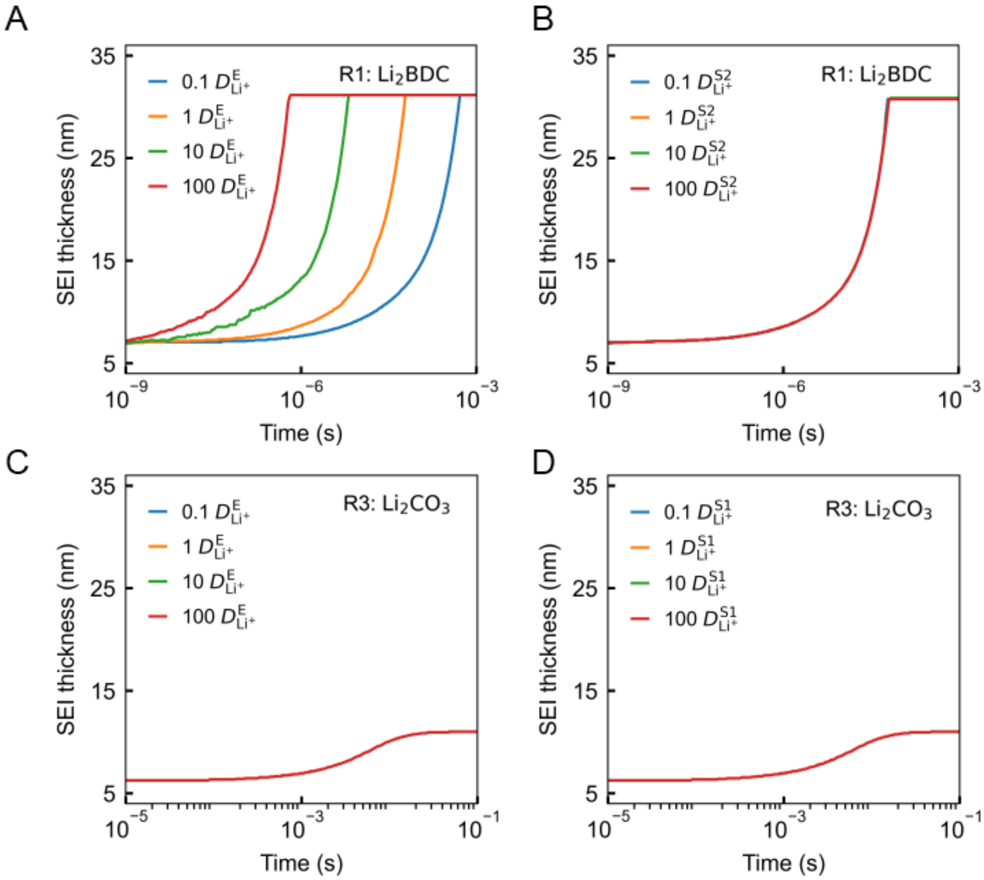

Fig. S9 Effect of the species diffusivity on SEI growth. Thickness evolution of dense organic Li_2BDC via R1 with varying Li^+ diffusivity in (A) liquid EC electrolyte and (B) the formed organic Li_2BDC. (C, D) Temporal evolution of thickness of dense inorganic Li_2CO_3 via R3 with varying Li^+ diffusivity in (C) liquid EC electrolyte and (D) the formed inorganic Li_2CO_3. The Li^+ diffusivity in liquid EC ($D_{Li^+}^{E}$= 3.5 × 10^{-10} m^2/s) was obtained from MD simulations and the Li^+ diffusivity in Li_2CO_3 ($D_{Li^+}^{S1}$ = 1.1 × 10^{-11} m^2/s) was calculated by DFT[3]. The Li^+ diffusivity in solid Li_2BDC ($D_{Li^+}^{S2}$ = 1.0 × 10^{-10} m^2/s) is estimated.

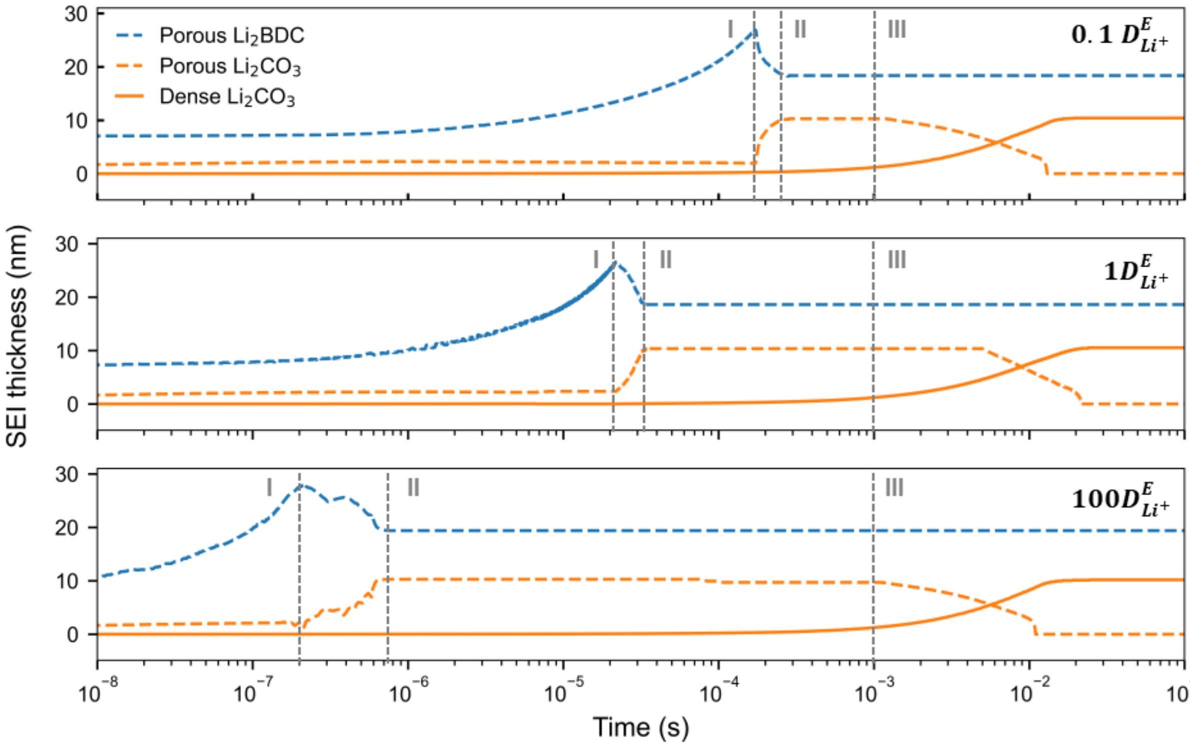

Fig. S10 Time-resolved SEI growth in the Li/(EC + 1 M $LiPF_6$) system with varying Li^+ diffusivity in electrolyte. The dashed and solid lines represent the porous and dense products, respectively. Stage I: Porous organic Li_2BDC forms via R1; State II: A portion of this Li_2BDC is converted to porous inorganic Li_2CO_3 through the R2 pathway. Stage III: The remaining pores are filled as additional Li_2CO_3 is produced by the direct two-electron reduction of EC via R3.

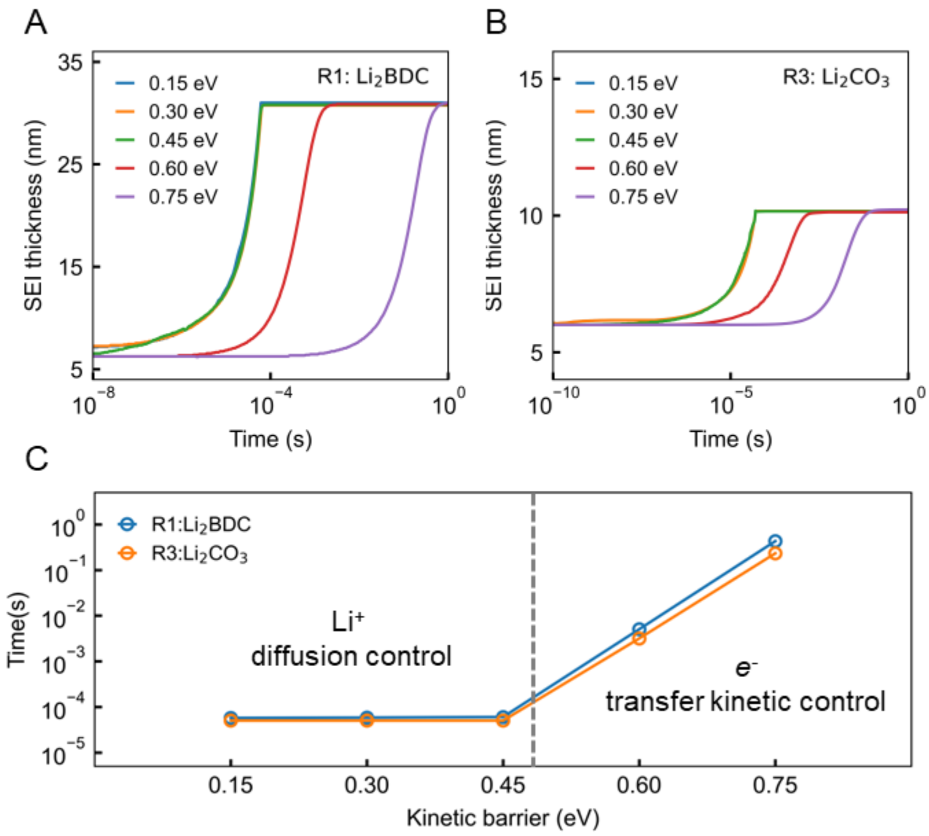

Fig. S11 Effect of the electron-transfer kinetic barrier (ΔG^*) on SEI growth. Thickness evolution of (A) dense organic Li_2BDC formed via R1 and (B) dense inorganic Li_2CO_3 formed via R3 with varying ΔG^*. (C) Time required for each SEI component to reach its tunneling-limited thickness. The intrinsic electron transfer barrier, 0.15 eV for Li_2BDC and 0.72 eV for Li_2CO_3, are obtained from DFT calculations, and a series of parameterized values are explored around these baselines to evaluate the impact of ΔG^*on SEI growth dynamics.

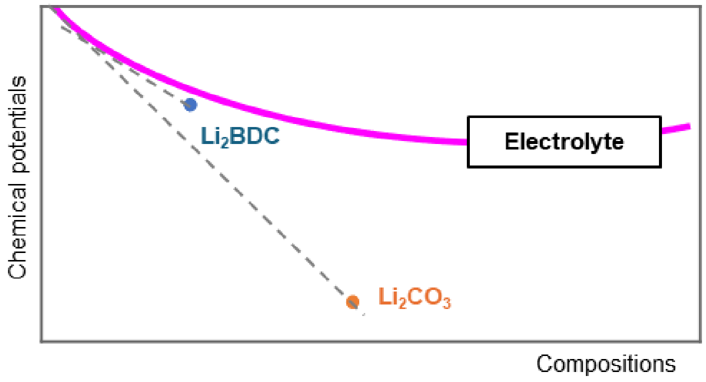

Fig. S12 Chemical potentials of phases.

Supplementary note: 1

Phase field model: For the Li metal – SEI – Electrolyte system with R1 to R3 in Fig. 2C and the Li plating/stripping reaction $Li^+ + e^- = Li$, the Gibbs free energy change dg per unit volume of such a system in terms of the changes in the total concentrations and the changes in the extent of the 4 reactions, ξ_m (*m*=0,1,2,3)

$$dg = \sum_{n=1}^{3} \tilde{\mu}_n dc_n^{tot} + c \sum_{m=0}^{3} \Delta G_m^r d\xi_m \tag{1}$$

where *n* (=1,2,3) represents Li$^+$, e$^-$, and EC, and ΔG_m^r are the Gibbs free energy difference between the products and reactants of reaction m:

$$\Delta G_m^r = \Delta G_m^0 + \mathcal{F}(\psi_e - \psi_{sol} - \psi_m^0) - RT \ln\left(\prod_k^{reactants} a_k^{v_k^m} \prod_l^{products} a_l^{v_l^m}\right) \tag{2}$$

Then, the correlations among the phase fractions $\phi^{M,S1,S2}$ and extents of reactions ξ_m as

$$\phi^M = \xi_0 \tag{3}$$

$$\phi^{S2} = \xi_1 - \xi_2 \tag{4}$$

$$\phi^{S1} = \xi_2 + \xi_3 \tag{5}$$

The total free energy *G* of the system is given by,

$$G = \int (g_{chem} + g_{int}) dV \tag{6}$$

where g_{chem} is the local bulk chemical free energy density of the system,

$$g_{chem} = h(\phi_E)\mu^E(\{x_n\}) + h(\phi_M)\mu_{Li}^o + h(\phi_{S1})\mu_{S1}^o + h(\phi_{S2})\mu_{S2}^o \tag{7}$$

here $h(\phi) = 6\phi^5 - 15\phi^4 + 10\phi^3$ is an interpolation function, $\mu^E(\{x_n\})$ is the chemical potential of the electrolyte solution, which is a continuous function of species compositions $x_n = c_n/c_0$, and μ_{Li}^{o}, μ_{S1}^{o} and μ_{S2}^{o} are standard chemical potentials of Li, Li_2CO_3 and Li_2BDC, respectively, which are functions of only temperature.

The interfacial energy contribution g_{int} by the interfaces among the four phases is introduced through a simple multi-well function and gradient terms,

$$g_{int} = g_{well} + g_{grad} \tag{8}$$

$$g_{well} = \sum_j\left[-w_j\left(2-\phi_j^2\right)\phi_j^2\right] + \sum_{j,l>j}\gamma_{jl}\phi_j^2\phi_l^2 \tag{9}$$

$$g_{grad} = \sum_j \frac{\kappa_j}{2}\left(\nabla\phi_j\right)^2 \tag{10}$$

where w_j is the height of the double-well, γ_{jl} are positive values to guarantee that the local minima of the multi-well function are located at $(\phi_E, \phi_M, \phi_{S1}, \phi_{S2}) = (1,0,0,0), (0,1,0,0), (0,0,1,0), (0,0,0,1)$, and κ_i represents the gradient coefficients. These three parameters can be quantified based on the interfacial energy and thickness for different types of interfaces. In this study, we assume all the interfacial energies are 0.5 J/m^2 and the interface thickness is 1 nm. In our future 2-D simulations, the interfacial energies will be taken from our previous DFT calculations.

Therefore, the governing equation for the order parameters can be expressed as

$$\frac{\partial\phi_j}{\partial t} = -L_j\frac{\delta G}{\delta\phi_j} \tag{11}$$

According to the correlation between phase fractions and extents of reactions in Eq. (10), this governing equation can be re-written as,

$$\frac{\partial\phi_E}{\partial t} = -L_E\left(\frac{\partial g_{well}}{\partial\phi_E} - \kappa_E\nabla^2\phi_E\right) \tag{12}$$

$$\frac{\partial \phi_M}{\partial t} = -L_M \left(\frac{\partial g_{well}}{\partial \phi_M} - \kappa_M \nabla^2 \phi_M \right) + h'(\phi_M) R_0 \tag{13}$$

$$\frac{\partial \phi_{S1}}{\partial t} = -L_{S1} \left(\frac{\partial g_{well}}{\partial \phi_{S1}} - \kappa_{S1} \nabla^2 \phi_{S1} \right) + h'(\phi_{S1})(R_2 + R_3) \tag{14}$$

$$\frac{\partial \phi_{S2}}{\partial t} = -L_{S2} \left(\frac{\partial g_{well}}{\partial \phi_{S2}} - \kappa_{S2} \nabla^2 \phi_{S2} \right) + h'(\phi_{S2})(R_1 - R_2) \tag{16}$$

where L_j is the interface mobility coefficient and R_m is the reaction rate:

$$R_m = -k_m \frac{\Delta G_m^r}{RT} \tag{17}$$

k_m can be formulated as $k_m = k_m^0 \exp\left(-\frac{\Delta G_m^*}{RT}\right)$ where $k_m^0 = \frac{k_B T}{h}$ is a prefactor and ΔG_m^* is the activation energy. k_B is Boltzmann constant, and h is Planck constant.

Reference

1. D. Bedrov, G. D. Smith and A. C. van Duin, *J. Phys. Chem. A.*, 2012, **116**, 2978-2985.
2. Z. Liu, Y. Li, Y. Ji, Q. Zhang, X. Xiao, Y. Yao, L.-Q. Chen and Y. Qi, *Cell Reports Physical Science*, 2021, **2**, 100294-100294.
3. S. Shi, P. Lu, Z. Liu, Y. Qi, L. G. Hector, H. Li and S. J. Harris, *Journal of the American Chemical Society*, 2012, **134**, 15476-15487.
4. Y. X. Lin, Z. Liu, K. Leung, L.-Q. Chen, P. Lu and Y. Qi, *Journal of Power Sources*, 2016, **309**, 221-230.
5. Z. Liu, Y. Qi, Y. X. Lin, L. Chen, P. Lu and L.-Q. Chen, *J. Electrochem. Soc.*, 2016, **163**, A592-A598.